



# Polyethyleneimine Incorporated Metal-Organic Frameworks Adsorbent for Highly Selective CO<sub>2</sub> Capture

Yichao Lin, Qiuju Yan, Chunlong Kong & Liang Chen

Ningbo Institute of Materials Technology and Engineering, Chinese Academy of Sciences, Ningbo, Zhejiang, 315201, P. R. China.

SUBJECT AREAS:

METAL-ORGANIC  
FRAMEWORKS

ATMOSPHERIC CHEMISTRY

POROUS MATERIALS

SOLID-STATE CHEMISTRY

Received  
4 April 2013

Accepted  
29 April 2013

Published  
17 May 2013

Correspondence and requests for materials should be addressed to L.C. (chenliang@nimte.ac.cn) or C.K. (kongchl@nimte.ac.cn)

A series of polyethyleneimine (PEI) incorporated MIL-101 adsorbents with different PEI loadings were reported for the first time in the present work. Although the surface area and pore volume of MIL-101 decreased significantly after loading PEI, all the resulting composites exhibited dramatically enhanced CO<sub>2</sub> adsorption capacity at low pressures. At 100 wt% PEI loading, the CO<sub>2</sub> adsorption capacity at 0.15 bar reached a very competitive value of 4.2 mmol g<sup>-1</sup> at 25 °C, and 3.4 mmol g<sup>-1</sup> at 50 °C. More importantly, the resulting adsorbents displayed rapid adsorption kinetics and ultrahigh selectivity for CO<sub>2</sub> over N<sub>2</sub> in the designed flue gas with 0.15 bar CO<sub>2</sub> and 0.75 bar N<sub>2</sub>. The CO<sub>2</sub> over N<sub>2</sub> selectivity was up to 770 at 25 °C, and 1200 at 50 °C. We believe that the PEI based metal-organic frameworks is an attractive adsorbent for CO<sub>2</sub> capture.

The rapidly increasing concentration of CO<sub>2</sub> in atmosphere, which mainly stem from the combustion of fossil fuels, is believed to be responsible for some severe global environmental crisis, such as climate change and ocean acidification. The capture and sequestration of CO<sub>2</sub> in an energy-efficient and economical manner is deemed as a solution to mitigate the CO<sub>2</sub> emission until a mature alternative new energy technology is sufficiently developed<sup>1</sup>. However, selective capture of CO<sub>2</sub> from flue gas emissions still remains challenging to date. One of the major bottlenecks is the absence of CO<sub>2</sub> adsorbent with high selectivity, rapid adsorption kinetics, high stability under practical conditions, high adsorption ability and low regeneration cost. Aqueous solutions of amines (20–30% concentration) are commonly used in large scale to capture CO<sub>2</sub> from industrial streams because they have large capacity and high selectivity for acidic gases<sup>2</sup>. However, high heat capacity of these aqueous solutions makes the regeneration very energy intensive and costly<sup>3</sup>. Instead, solid porous adsorbents are emerging as more promising candidates because the much lower heat capacity of solids can significantly reduce the regeneration energy cost. In addition, the corrosion and volatility issues, which are intrinsic to amine solutions, could be minimized in solid adsorbents.

Recently, solid metal-organic frameworks (MOFs) adsorbents have received a great deal of attention because they exhibit remarkable CO<sub>2</sub> adsorption capacity at high pressures owing to their extremely high surface areas and porosity<sup>4–8</sup>. However, the CO<sub>2</sub> adsorption capacities of most MOFs are unsatisfying at low pressures, especially below 0.15 bar, the condition relevant to practical applications. Some attempts have been made to enhance the CO<sub>2</sub> capture ability for MOFs at low pressure, such as developing MOFs with amine-functionality<sup>9,10</sup>. Apparently, the basic amine group is an ideal functionality to strongly interact with acidic CO<sub>2</sub> molecules. However, amine-functionalized MOFs have been shown to be not very successful in CO<sub>2</sub> capture. It was proposed that the covalent grafting of amine groups to the aromatic rings in MOFs cannot significantly enhance the affinity of CO<sub>2</sub> on amine groups because of the electron withdrawing effect of benzene ring<sup>11</sup>. Alternatively, some recent studies on incorporation of diamine to the open metal sites of MOFs have been shown to dramatically enhance CO<sub>2</sub> capture at low pressures. The open metal sites play an important role to anchor one end of the diamine groups and leave the other end (alkylamines) available to capture CO<sub>2</sub>. Here we anticipate that physical impregnation of poly-alkylamines into MOFs would afford more active amine groups than diamines and maintain the strong interaction between CO<sub>2</sub> and alkylamine groups. Among the polyamines, polyethyleneimine (PEI) is one of the best candidates to bind CO<sub>2</sub> due to its high amine density and accessible primary amine sites on the chain ends<sup>12,13</sup>. Indeed, some recent studies reported that PEI based silica and zeolite have excellent CO<sub>2</sub> capture ability<sup>3,12,14–16,9</sup>. Ideally, the much higher pore volume, porosity and surface area of MOFs than silica or zeolite make them even more competent media to impregnate PEI for CO<sub>2</sub> capture. However, to date, no impregnation

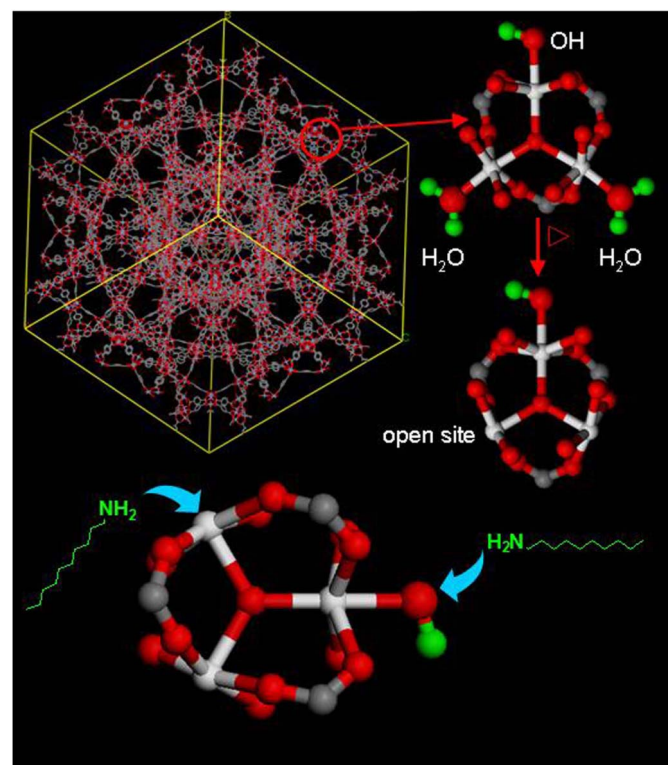


of PEI into MOFs has been reported. This is partly because the complexity of MOFs including pore size and porosity would make it difficult to efficiently load PEI into the MOF pores.

In this study, we report a series of PEI modified MOF adsorbents with low molecular-weight linear PEI loaded into MIL-101(Cr)<sup>17</sup> for highly efficient CO<sub>2</sub> capture. We chose MIL-101(Cr) as the model system for MOFs because it has very large surface area (above 3000 m<sup>2</sup> g<sup>-1</sup>), high porosity, excellent thermal and chemical stability, as well as high resistance to moisture. In addition, MIL-101(Cr) possesses open metal sites, which can serve as Lewis acid to anchor the Lewis basic amine groups of PEI<sup>18,19</sup>, while leave other alkylamine groups available as reactive adsorption sites to capture CO<sub>2</sub> (see Figure 1). Moreover, we expect that the Cr-OH groups in MIL-101 may also anchor the amine groups. Thus, the loaded PEI can interact strongly with the pore wall of MIL-101(Cr) after the removal of solvent. Considering that short-chain and linear PEI can pass the relatively narrow MIL-101 pore windows (with diameters of 1.2–1.6 nm) more smoothly, low-molecular-weight linear PEI was chosen. As a result, solid and porous PEI-MIL-101 adsorbents with moderate surface areas were successfully assembled.

## Results

**Characterization of PEI-MIL-101.** PEI-MIL-101 with different PEI loadings, corresponding to 50%, 75%, 100% and 125%, were prepared and characterized by the combination of PXRD, SEM, IR, TGA and N<sub>2</sub> adsorption/desorption at 77 K measurements. As shown in the PXRD patterns (Figure S1), the Bragg diffraction angles in MIL-101 and PEI-MIL-101 with different PEI loadings were essentially identical, confirming that the MIL-101 crystalline structure was preserved after loading PEI. However, we observed that the intensity of the peaks below 7° was largely reduced as the PEI loading increased. In particular, the peak at 3.44°, corresponding to the (2 2 2) plane of MIL-101, was nearly invisible in PEI-MIL-101-125. These changes are ascribed to the filling of MIL-101 pores, and indicate that PEI is not simply coated on the outer surface of MIL-101. Actually, similar phenomenon has also been observed on the SBA-15 supported PEI<sup>12</sup>.



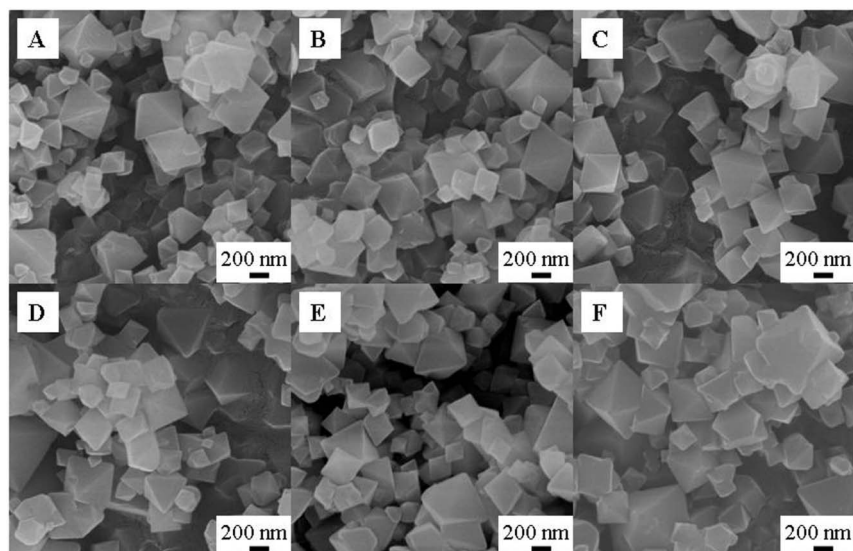
**Figure 1** | The illustration of the interactions between PEI and MIL-101.

Figure 2 shows the morphologies of MIL-101 before and after loading PEI. The MIL-101 octahedral particle size was rather small (with diameters of 100–500 nm), which can sufficiently facilitate the diffusion of PEI into the MIL-101 pores. Indeed, after loading the PEI, no particle stacking was found, even at 160% loading, indicating that PEI was really loaded into MIL-101 pores. In addition, the morphologies and sizes of MIL-101 after loading the PEI remained nearly intact. To some extent, it also suggested that the MIL-101 structure was preserved after loading PEI.

To ensure the presence of PEI and detect the interactions between PEI and MIL-101, IR spectra were collected on activated PEI-MIL-101 under vacuum condition. As shown in Figure 3, the representative peaks between 3500–2800 cm<sup>-1</sup> corresponding to ν(NH) and ν(CH) stretching vibrations can be clearly observed in the IR of PEI-MIL-101 samples, which were consistent with that of pure PEI sample. The N-H bending vibration was also discernable at 1570 cm<sup>-1</sup> (Figure S2). The band at 3620 cm<sup>-1</sup>, which can be assigned to Cr-OH<sup>20</sup>, was clearly observed in MIL-101. Notably, after PEI loading, this band completely disappeared. It indicated a chemical interaction between the Cr-OH groups and PEI amines, and possible formation of Cr-O-NH<sub>3</sub>R<sup>3</sup>. In addition, it was reported that amine groups can bind to open Cr sites, resulting in a slight blue-shift of C-H stretching vibration adjacent to the interacting amine groups. However, in the present study, the abundant C-H groups not adjacent to the interacting amine groups would make it hard to detect the slight blue-shift of C-H stretching vibration. Nevertheless, we believe that open metal sites still play an important role to glue PEI on the MIL-101 surface.

TGA measurement was employed to evaluate the thermal stability of MIL-101 before and after loading PEI (Figure S3). Interestingly, when PEI was loaded into MIL-101, the sharp weight loss of PEI took place at higher temperatures (~225°C). Moreover, the stability of MIL-101 was also increased slightly. It suggested that the strong interactions between PEI and MIL-101, most likely on the open Cr sites and Cr-OH groups, were formed and enhanced the stability of PEI-MIL-101 composite. Indeed, no elevated decomposition temperature of PEI was found when silica was used as the support<sup>21</sup>. However, incorporation of Zr into the silica support can dramatically stabilize the PEI-silica composite<sup>12</sup>.

The N<sub>2</sub> adsorption/desorption isotherms of MIL-101 at 77 K before and after loading PEI were measured to evaluate their surface area and pore volume. As shown in Figure 4, the original MIL-101 exhibited very high N<sub>2</sub> uptakes with a saturated uptake of 1000 cm<sup>3</sup> g<sup>-1</sup>, which was well consistent with the values in literatures<sup>22,23</sup>. The corresponding BET surface area and pore volume were calculated to be 3225 m<sup>2</sup> g<sup>-1</sup> and 1629 cm<sup>3</sup> g<sup>-1</sup>, respectively. After PEI was loaded into MIL-101, the N<sub>2</sub> uptake, surface area and pore volume decreased dramatically. As shown in Figure 5 and Table 1, the saturated N<sub>2</sub> uptake, surface area and pore volume of PEI-MIL-101-50 were roughly half that of pure MIL-101. Particularly, the reduced pore volume confirmed that the PEI was loaded into MIL-101 pores. When the PEI loading was continuously increased to 125 wt%, the saturated N<sub>2</sub> uptake drastically dropped to only 50 cm<sup>3</sup> g<sup>-1</sup>. Since the pore volume of the bare MIL-101 is 1.629 cm<sup>3</sup> g<sup>-1</sup> and the density of PEI is 1.0 g/ml, the theoretical maximum PEI loading in MIL-101 pores should be approximately 160 wt%. Indeed, in the prepared PEI-MIL-101-160 sample, the resulting surface area and pore volume were only 7.4 m<sup>2</sup> g<sup>-1</sup> and 0.019 cm<sup>3</sup> g<sup>-1</sup> (Figure S4), respectively, indicating the complete pore filling of MIL-101 by PEI. Clearly, such material is incapable for gas adsorption. Therefore, in the following gas adsorption experiments, we discarded the PEI-MIL-101-160 sample and focused on the PEI-MIL-101 with 50–125 wt% loadings. Nevertheless, to the best of our knowledge, 125 wt% PEI (and correspondingly amine groups) is already the highest amount that can be loaded into the porous materials. It was expected that the more amount of PEI loaded would result in higher CO<sub>2</sub> adsorption capacity<sup>24,25</sup>.



**Figure 2** | The SEM images of (A) original MIL-101, (B) PEI-MIL-101-50, (C) PEI-MIL-101-75, (D) PEI-MIL-101-100, (E) PEI-MIL-101-125 and (F) PEI-MIL-101-160.

**CO<sub>2</sub> uptake.** The CO<sub>2</sub> isotherms of MIL-101 and PEI-MIL-101 samples obtained at low-pressures and 25°C are presented in Figure 5. All isotherms were fitted with the Langmuir-Freundlich model<sup>26–28</sup>. It can be seen that all PEI-MIL-101 samples exhibited significantly enhanced CO<sub>2</sub> adsorption compared to the original MIL-101. At 1 bar, PEI-MIL-101-50 can adsorb 4.0 mmol g<sup>-1</sup> of CO<sub>2</sub>, representing a ~150% improvement in gravimetric capacity relative to MIL-101. When the PEI loading was increased to 75 and 100 wt%, the CO<sub>2</sub> adsorption uptake was further enhanced at all tested pressures. An outstanding uptake of 5.0 mmol g<sup>-1</sup> was achieved at 1 bar, which is on par with that of recently reported MOFs appended with diamines<sup>29,30</sup>. However, when the PEI loading was further increased to 125 wt%, decreased CO<sub>2</sub> adsorption uptakes were found. The PEI-MIL-101-125 can adsorb 4.35 mmol g<sup>-1</sup> of CO<sub>2</sub> at 1 bar, about 13% lower than that of

PEI-MIL-101-100. At higher pressure, the decrease is even more significant. Actually, as aforementioned, the surface areas of PEI-MIL-101-125 dropped to only 182.9 m<sup>2</sup> g<sup>-1</sup>, indicating that some pores were completely filled and thus not accessible to CO<sub>2</sub> molecules at room temperature. Furthermore, incorporation of PEI into MIL-101 would increase the framework density, which is also negative to the improvement in CO<sub>2</sub> gravimetric capacity. Although we do not show the data at higher pressures (>2 bar), but the trend can be clearly seen that the adsorption uptake at higher pressures would follow the sequence: MIL-101 > PEI-MIL-101-50 > PEI-MIL-101-75 > PEI-MIL-101-100 > PEI-MIL-101-125 (i.e., proportional to the surface area). Therefore, it is necessary to carefully balance the PEI loading and adsorbents surface area to achieve the desired CO<sub>2</sub> adsorption capacity at specific pressures.

To investigate the influence of elevated temperature on CO<sub>2</sub> adsorption behaviors of the PEI-MIL-101 adsorbents, we further measured the CO<sub>2</sub> adsorption isotherms of the PEI-MIL-101 samples at 50°C (Figure S5). Interestingly, at 50°C, PEI-MIL-101-125 displayed the highest CO<sub>2</sub> uptakes at all tested pressures. Moreover, the CO<sub>2</sub> adsorption capacity of PEI-MIL-101-125 at 50°C was also higher than its adsorption capacity at 25°C. Actually, a similar phenomenon has also been observed when PEI was loaded into SBA-15<sup>3</sup>. Indeed, due to the high elasticity of PEI, some pores in PEI-MIL-101-125 that were not accessible to CO<sub>2</sub> molecules at low temperature, would become accessible at elevated temperatures. Furthermore, the high kinetic barrier for the diffusion of CO<sub>2</sub> from the surface into the filled pores would be overcome by the intense thermal motion at higher temperature. Apparently, upon PEI impregnation, the original window size (1.2–1.6 nm) and pore size (2.9–3.4 nm) of MIL-101 were reduced so that CO<sub>2</sub> diffusion would be more difficult. On the other hand, it is worth mentioning that the small and unstacked PEI-MIL-101 particles in this study would sufficiently facilitate the diffusion of CO<sub>2</sub> from the gas phase to the surface and inner pores of the sorbents.

Above we discussed the CO<sub>2</sub> adsorption uptakes of PEI-MIL-101 materials at 1 bar. Actually, the CO<sub>2</sub> uptake at near 0.15 bar is a more important parameter because the flue gas usually contains ~15% CO<sub>2</sub><sup>31</sup>. Hence, the CO<sub>2</sub> adsorption uptakes of the PEI-MIL-101 samples at 0.15 and 1 bar are summarized in Table 1 for comparison. Fortunately, it is found that the CO<sub>2</sub> adsorption uptakes of PEI-MIL-101 increase extremely fast with respect to pressure in the range of 0–0.2 bar, which make them very advantageous for low-pressure CO<sub>2</sub>

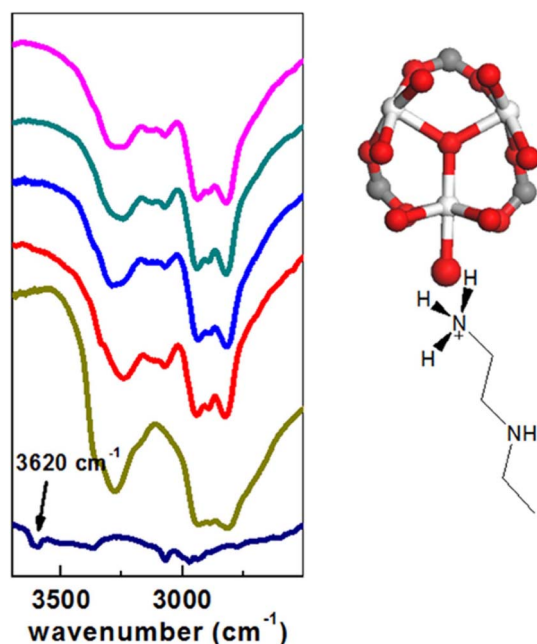


**Figure 3** | IR spectra of the pure PEI and MIL-101 before and after loading PEI. From bottom to top: MIL-101, pure PEI, PEI-MIL-101-50, PEI-MIL-101-75, PEI-MIL-101-100, PEI-MIL-101-125.



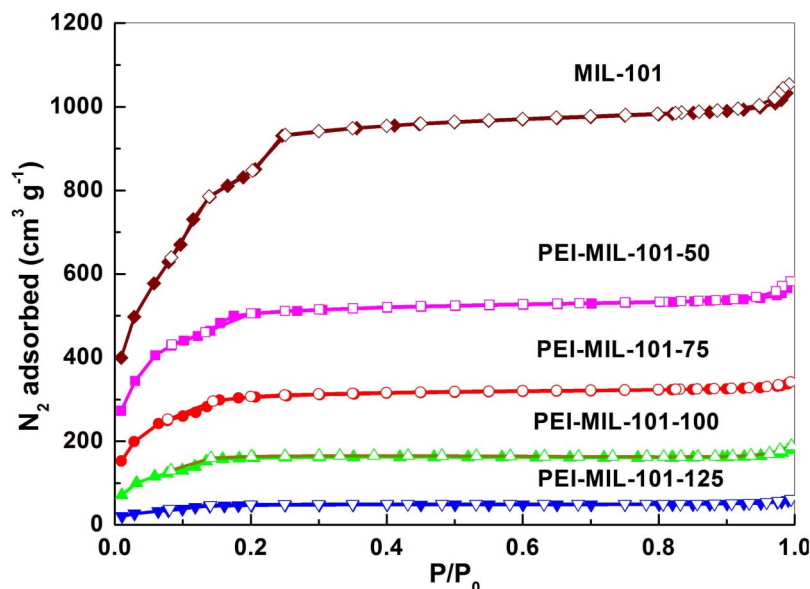


Figure 4 |  $N_2$  adsorption-desorption isotherms at 77 K. The symbols: Filled, adsorption; Blank, desorption.

capture. On the PEI-MIL-101 samples with higher loadings ( $>75$  wt%),  $CO_2$  uptakes rapidly reached a considerable amount at 0.15–0.2 bar. At 0.15 bar and  $25^\circ C$ , PEI-MIL-101-100 displayed the best  $CO_2$  adsorption performance with a value of  $4.2 \text{ mmol g}^{-1}$ . Under the same conditions, the original MIL-101 can only capture  $0.33 \text{ mmol g}^{-1} CO_2$ , respectively. Thus, PEI-MIL-101-100 can adsorb about 12 times more  $CO_2$ , even though the surface is reduced by 80%. The capacity value of PEI-MIL-101-100 is  $\sim 220\%$  higher than the saturation absorption capacity ( $1.32 \text{ mmol g}^{-1} CO_2$ ) of 30% MEA solution at  $25^\circ C$  and 0.15 bar, which is commonly used in coal-fired power plants<sup>2,29,32</sup>. Very recently, PEI/Zr-SBA-15 was reported to show excellent  $CO_2$  adsorption performance, with a  $CO_2$  capacity of  $1.65 \text{ mmol g}^{-1}$  at a partial pressure of 0.1 bar and  $25^\circ C$ . Here, at 0.1 bar and  $25^\circ C$ , PEI-MIL-101-100 can adsorb about 140% more amount ( $4.0 \text{ mmol g}^{-1}$ ) of  $CO_2$  owing to the higher loading of PEI. The performance of PEI-MIL-101-100 for  $CO_2$  capture at 0.15 bar is on par with that of the best functionalized solid materials reported to date, particularly the MOF-based materials<sup>3,29,30,33,34</sup>. In addition, we

also measured the  $CO_2$  adsorption capacity of humid PEI-MIL-101-100, which was exposed to moisture. No decreased  $CO_2$  adsorption capacity was observed, indicating the high moisture stability of the PEI-MIL-101 materials.

**$CO_2$  adsorption Kinetics and cycling measurements.** As mentioned, one of the major bottlenecks for deliverable  $CO_2$  adsorbents is the slow adsorption kinetics. Thus, it is very necessary to measure the  $CO_2$  adsorption kinetics of PEI-MIL-101 materials. As shown in Figure 6,  $CO_2$  adsorption capacity in PEI-MIL-101-100 could reach  $4.2 \text{ mmol g}^{-1}$  within the first 5 minutes. Afterwards, the PEI-MIL-101-100 sample seemed completely saturated. The corresponding pressure drop (to around 0.15 bar) in the sample holder also indicated a very rapid adsorption behavior (Figure S7). The  $CO_2$  adsorption kinetics for PEI-MIL-50, 75 and 125 (Figure S8–S10) were similar to that of PEI-MIL-101-100. Hence, PEI-MIL-101 materials exhibited rather good kinetics for  $CO_2$  adsorption.

To ensure the regenerability of PEI-MIL-101 materials, we further performed  $CO_2$  adsorption cycling measurements. In our experiments, we found that the  $CO_2$  captured in PEI-MIL-101 materials can be completely desorbed at  $110^\circ C$  under vacuum condition for 1 hour, which is confirmed by the equal mass of PEI-MIL-101 materials before adsorption and after desorption measurements (Table S1). Therefore, between each cycle measurement, the sample was degassed at  $110^\circ C$  for 1 hour under vacuum condition. It can be obviously observed that, after five adsorption/desorption cycles, the  $CO_2$  adsorption capacity of the prepared PEI-MIL-101 was well retained.

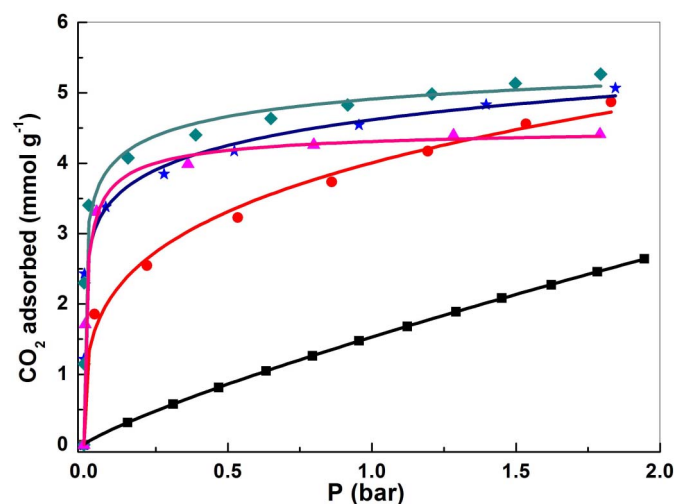


Figure 5 | The  $CO_2$  adsorption isotherms of the MIL-101 before and after loading PEI at  $25^\circ C$ . Symbol: ■ MIL-101, ● PEI-MIL-101-50, ★ PEI-MIL-101-75, ◆ PEI-MIL-101-100, ▲ PEI-MIL-101-125. Lines are the fitted isotherms.

**$CO_2/N_2$  selectivity.** Motivated by the observation that increasing PEI loading would reduce the  $N_2$  adsorption uptake but enhance  $CO_2$  adsorption uptake, we anticipate that this kind of materials could be an exceptional candidate for post-combustion  $CO_2$  capture. For coal-fired power stations, the main flue gas components by volume are  $N_2$  ( $\sim 75\%$ ) and  $CO_2$  ( $\sim 15\%$ ). Thus, the  $CO_2$  selectivity for a gas mixture with 0.15 bar  $CO_2$  and 0.75 bar  $N_2$  is often used to evaluate the  $CO_2$  capture ability. Therefore, the adsorption isotherms for  $N_2$  in MIL-101 before and after loading the PEI were also measured (Fig S11–12), and the molar selectivity of MIL-101 before and after loading the PEI in the designed gas mixture were further calculated according to the previously reported equation<sup>29,30,35</sup>. Similar to the  $N_2$  adsorption at 77 K, PEI-MIL-101 adsorbed less  $N_2$  than pure



Table 1 | The measured properties of the PEI-MIL-101 adsorbents at 0.15 and 1 bar

	PEI loading (wt%)	$S_{BET}$ ( $m^2 g^{-1}$ )	$V_{total}$ ( $cm^3 g^{-1}$ )	Occupancy $^a$ (%)	$CO_2$ adsorbed ( $mmol g^{-1}$ )			
					25°C		50°C	
					0.15 bar	1 bar	0.15 bar	1 bar
MIL-101	0	3125.4	1.629	0	0.33	1.60	0.20	1.00
PEI-MIL-101-50	50	1802.7	0.901	31	2.40	4.00	1.86	3.07
PEI-MIL-101-75	75	1112.6	0.526	46	3.67	4.64	3.17	4.02
PEI-MIL-101-100	100	608.4	0.292	61	4.20	5.00	3.40	4.14
PEI-MIL-101-125	125	182.9	0.095	77	3.85	4.35	3.95	4.51

<sup>a</sup>The total volume of MIL-101 divided by the volume of loaded PEI, the density of PEI was 1 ml/g.

MIL-101 at all tested pressures and temperatures due to the significantly reduced surface area. Figure 7 depicts the calculated  $CO_2/N_2$  selectivities at 25 and 50°C. Indeed, PEI-MIL-101 materials show dramatically enhanced  $CO_2/N_2$  selectivities. For example, the  $CO_2/N_2$  selectivities for PEI-MIL-101-100 were calculated to be 600 at 25°C, 750 at 50°C. Further, the  $CO_2/N_2$  selectivities for PEI-MIL-101-125 reached 770 at 25°C, 1200 at 50°C. To the best of our knowledge, these values represent the highest  $CO_2/N_2$  selectivity in flue gas by zeolite and MOF-based adsorbents reported in literatures.

In addition, the mole of  $CO_2$  adsorbed at 0.15 bar divided by the mole of  $N_2$  adsorbed at 0.75 bar is also often employed to evaluate  $CO_2/N_2$  selectivity. Therefore, the corresponding  $CO_2/N_2$  selectivities for the PEI-MIL-101 materials were calculated using this method (Table S2). The calculated selectivities at 25°C for PEI-MIL-101-100 and PEI-MIL-101-125 were 120 and 150, respectively, both of which are much higher than that of PPN-6- $SO_3Li^{34}$  (selectivity = 17) and metal-inserted MOF-253<sup>33</sup> (selectivity = 12).

The separation performance of PEI-MIL-101 material for  $CO_2/N_2$  was further tested in a breakthrough experiment performed at 25°C using an equimolar  $CO_2/N_2$  mixture. As shown in Figure S13,  $N_2$  eluted rapidly from the column, whereas  $CO_2$  only started to elute after a period of time. Clearly, the distinct breakthrough data of the two components suggested the strong interaction between  $CO_2$  and PEI-MIL-101 materials and corroborated the high  $CO_2/N_2$  selectivity calculated from single component gas adsorption.

## Discussion

In conclusion, the impregnation of PEI into MOFs afforded a new and high-performance sorbent for post-combustion  $CO_2$  capture at

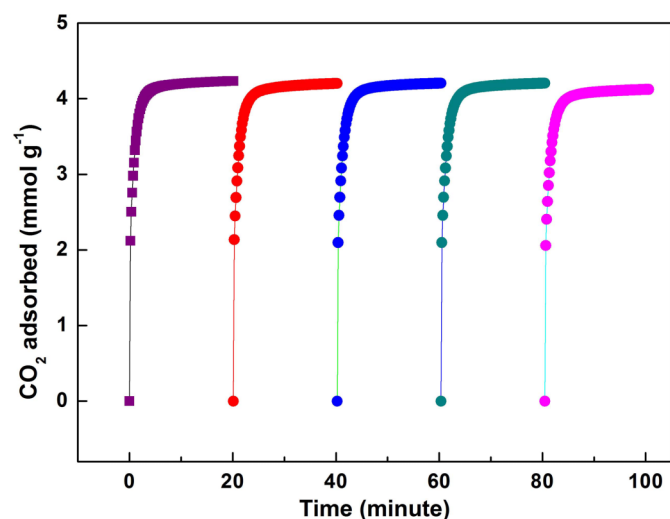


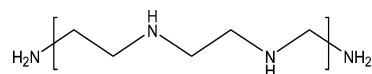
Figure 6 | Cycling  $CO_2$  adsorption kinetics of PEI-MIL-101-100. For clarity, the kinetics for the cycle 2, 3, 4 and 5 were shifted horizontally by 20, 40, 60 and 80.

low pressures. It possesses excellent  $CO_2$  adsorption capacity, rapid adsorption kinetics, together with very high  $CO_2/N_2$  selectivity in flue gas. We believe that PEI modified MOF is a more promising MOF-based material, considering that many pure MOF adsorbents are unsatisfying at low pressures, especially below 0.15 bar, which greatly hinders the practical application. Overall, the present study has demonstrated the first successful combination of polymeric amine and MOFs for post-combustion  $CO_2$  capture. We anticipate that some others MOFs with large surface area and open metal sites, such as NU-100<sup>36</sup> and MOF-177<sup>37</sup>, can also be excellent supports for PEI.

## Methods

**Materials.** The chemicals are of analytical grade and used without further purification in this study. Deionized water and alcohol was employed as solvent. The PEI (purity, 99%) used in the present study was a linear polymer with an average molecular weight of 300 g/mol. Due to the hygroscopic property, the PEI was placed in glove box.

The PEI molecular formula:



**Synthesis of MIL-101.** MIL-101 was prepared by a hydrothermal reaction following the procedure reported by Ferey and coworkers with minor difference: the hydrofluoric acid was replaced with hydrochloric acid. The detailed synthesis was as follows: chromic nitrate (800 mg, 2 mmol), terephthalic acid (332 mg, 2 mmol), 12 M hydrochloric acid (164  $\mu$ L, 2 mmol), and deionized water (10 ml) were mixed in a Teflon-lined stainless steel autoclave and kept at 220°C for 8 h. After the synthesis, the autoclave reactor was slowly cooled down to room temperature for 3 h in order to obtain larger crystals of the unreacted terephthalic acid. After cooling, the reaction mixture was filtered using a large pore paper filter to eliminate the recrystallized free acid. Water and MIL-101(Cr) powder can pass through the filter, whereas the free acid would stay inside or on the paper filter. After that, the product was recovered by centrifugation. To remove the free acid lying in the MIL-101(Cr)

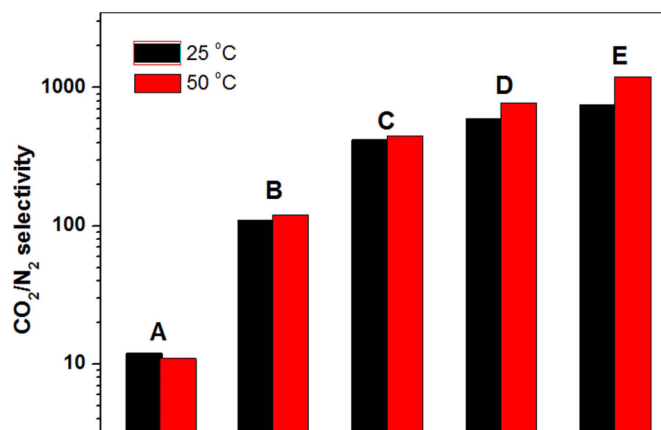


Figure 7 | The  $CO_2/N_2$  ideal selectivity for a gas mixture with 0.15 bar  $CO_2$  and 0.75 bar  $N_2$ . (A) MIL-101, (B) PEI-MIL-101-50, (C) PEI-MIL-101-75, (D) PEI-MIL-101-100, (E) PEI-MIL-101-125.



pores, a solvothermal treatment of the product was employed by using hot ethanol (95% EtOH, 5% water) in an autoclave at 80 °C for 8 h. The resulting solid was cooled down, centrifuged, and finally dried overnight at 80 °C under air atmosphere. For the following experiments, about 2 g MIL-101(Cr) samples were prepared by the above procedure.

**Synthesis of PEI-MIL-101 adsorbent.** The PEI-MIL-101 adsorbent was prepared by wet impregnation method. The detailed process was as follows. First, before the impregnation, the MIL-101 (Cr) powders were heated at 160 °C under vacuum condition for 12 h, removing the adsorbed water and coordinated water. Second, the desired amount of PEI was dissolved in 1 mL anhydrous methanol under stirring for 10 min, and then 0.2 g MIL-101 (Cr) powders were added step by step into the PEI/methanol solution under stirring. Finally, the resulting gel was dried overnight under room temperature and nitrogen protection, and then the temperature of the sample was increased at programmed rate and held at 110 °C for 12 h under vacuum condition. After that, a porous and solid PEI-MIL-101 (Cr) adsorbent was obtained. Herein, four PEI-MIL-101 samples with different PEI loadings were prepared, corresponding to 50%, 75%, 100% and 125%. To confirm the accurate PEI loading, the mass of MIL-101(Cr) was measured immediately after activated, and the mass of PEI was measured in glove box. The loading of PEI was calculated by the following equation:

$$\text{PEI loading} = \frac{\text{mass}_{\text{PEI}}}{\text{mass}_{\text{MIL-101}}} \times 100\% \quad (1)$$

In addition, the PEI loading amount was further verified by element analysis (see Table S3).

**Gas adsorption measurement.** The adsorption isotherms and of the probe gas CO<sub>2</sub> (purity, 99.999%) and N<sub>2</sub> (purity, 99.999%) were measured using volumetric technique by an apparatus from SETARAM France (PCTpro-E&E). Before each measurement, the sample was evacuated at 110 °C for 12 h. Pressure as a function of the amount of CO<sub>2</sub> adsorbed was determined using the Langmuir-Freundlich fit<sup>26–28</sup> for the isotherms:

$$\frac{N}{N_m} = \frac{B \times P^{(1/t)}}{1 + B \times P^{(1/t)}} \quad (2)$$

Here,  $N$  is the amount of CO<sub>2</sub> adsorbed (mmol g<sup>-1</sup>),  $p$  is the pressure,  $N_m$  is the amount of CO<sub>2</sub> adsorbed at saturation,  $B$  and  $t$  are constants. To solve the exact pressures,  $p$ , corresponding to constant amount of CO<sub>2</sub> adsorbed, the above equation can be rearranged to:

$$P = \left( \frac{N/N_m}{B - B \times N/N_m} \right)^t \quad (3)$$

**CO<sub>2</sub> selectivity calculations.** The CO<sub>2</sub> selectivities ( $S$ ) of samples were evaluated by the following equation which was previously reported<sup>29,30,35</sup>:

$$S = \frac{q_{\text{CO}_2} / p_{\text{CO}_2}}{q_{\text{N}_2} / p_{\text{N}_2}} \quad (4)$$

where  $q_i$  is the adsorption capacity of  $i$  component,  $p_i$  is the partial pressure of  $i$  component. The adsorption capacities of the components are defined to be molar excess adsorption capacities determined without correction for absolute adsorption.

**CO<sub>2</sub> adsorption kinetics measurement.** The CO<sub>2</sub> adsorption kinetics of the probe gas CO<sub>2</sub> were also measured using volumetric technique by the apparatus from SETARAM France (PCTpro-E&E). Before each measurement, the sample was evacuated at 110 °C for 12 h. In a simple procedure, the apparatus first give a desired pressure CO<sub>2</sub> gas to the sample holder, and record the pressure values in the sample holder and calculated the adsorbed CO<sub>2</sub> amount.

**Thermogravimetric analysis (TGA).** Thermogravimetric analysis (TGA) was measured using a system provided by Mettler Toledo (model TGA/DSC1), in air at a heating rate of 5 °C/min up to 600 °C. Before the TGA measurement, the samples were first activated and then placed in atmosphere for the same time (~5 days). The PEI was immediately measured after moving from the glove box.

**Infrared spectra (IR).** IR of the samples were recorded on KBr/sample pellets in a Thermo Nicolet 6700 spectrometer to determine the amine. IR spectra were collected on activated PEI-MIL-101 and MIL-101 samples under vacuum condition. IR spectra of pure PEI are also shown for comparison.

**Other physical measurements.** For structure analysis, powder x-ray diffraction (PXRD) data of the samples was collected on a Bruker AXS D8 Advance diffractometer using Cu K $\alpha$  radiation at room temperature. The 77 K nitrogen adsorption/desorption isotherm was measured on ASAP 2020 M apparatus. The Brunauer-Emmett-Teller (BET) surface area was calculated over the range of relative pressures between 0.05 and 0.20 bar. Before the 77 K N<sub>2</sub> adsorption/desorption measurements, samples were pretreated under vacuum at 110 °C for 12 h. The as-prepared samples morphologies were examined using a field emission scanning electron microscope (SEM) (Hitachi, S-4800).

- Haszeldine, R. S. Carbon Capture and Storage: How Green Can Black Be? *Science* **325**, 1647–1652 (2009).
- Rochelle, G. T. Amine Scrubbing for CO<sub>2</sub> Capture. *Science* **325**, 1652–1654 (2009).
- Ma, X. L., Wang, X. X. & Song, C. S. "Molecular Basket" Sorbents for Separation of CO<sub>2</sub> and H<sub>2</sub>S from Various Gas Streams. *J. Am. Chem. Soc.* **131**, 5777–5783 (2009).
- Kauffman, K. L. *et al.* Selective Adsorption of CO<sub>2</sub> from Light Gas Mixtures by Using a Structurally Dynamic Porous Coordination Polymer. *Angew. Chem. Int. Edit.* **50**, 10888–10892 (2011).
- Sumida, K. *et al.* Carbon Dioxide Capture in Metal-Organic Frameworks. *Chem. Rev.* **112**, 724–781 (2012).
- Llewellyn, P. L. *et al.* High uptakes of CO<sub>2</sub> and CH<sub>4</sub> in mesoporous metal-organic frameworks MIL-100 and MIL-101. *Langmuir* **24**, 7245–7250 (2008).
- Furukawa, H. *et al.* Ultrahigh Porosity in Metal-Organic Frameworks. *Science* **329**, 424–428 (2010).
- Babarao, R., Jiang, J. W. & Sandler, S. I. Molecular Simulations for Adsorptive Separation of CO<sub>2</sub>/CH<sub>4</sub> Mixture in Metal-Exposed, Catenated, and Charged Metal-Organic Frameworks. *Langmuir* **25**, 6590–6590 (2009).
- Lin, Y. C., Kong, C. L. & Chen, L. Direct synthesis of amine-functionalized MIL-101(Cr) nanoparticles and application for CO<sub>2</sub> capture. *RSC Adv.* **2**, 6417–6419 (2012).
- Si, X. L. *et al.* High and selective CO<sub>2</sub> uptake, H<sub>2</sub> storage and methanol sensing on the amine-decorated 12-connected MOF CAU-1. *Energy Environ. Sci.* **4**, 4522–4527 (2011).
- Brune, S. N. & Bobbitt, D. R. Role of Electron-Donating Withdrawing Character, Ph, and Stoichiometry on the Chemiluminescent Reaction of Tris(2,2'-Bipyridyl)Ruthenium(II) with Amino-Acids. *Anal. Chem.* **64**, 166–170 (1992).
- Kuwahara, Y. *et al.* Dramatic Enhancement of CO<sub>2</sub> Uptake by Poly(ethyleneimine) Using Zirconosilicate Supports. *J. Am. Chem. Soc.* **134**, 10757–10760 (2012).
- Chaikititilp, W., Khunsupat, R., Chen, T. T. & Jones, C. W. Poly(allylamine)-Mesoporous Silica Composite Materials for CO<sub>2</sub> Capture from Simulated Flue Gas or Ambient Air. *Ind. Eng. Chem. Res.* **50**, 14203–14210 (2011).
- Goepfert, A. *et al.* Carbon Dioxide Capture from the Air Using a Polyamine Based Regenerable Solid Adsorbent. *J. Am. Chem. Soc.* **133**, 20164–20167 (2011).
- Qi, G. G., Fu, L. L., Choi, B. H. & Giannelis, E. P. Efficient CO<sub>2</sub> sorbents based on silica foam with ultra-large mesopores. *Energy Environ. Sci.* **5**, 7368–7375 (2012).
- Qi, G. G. *et al.* High efficiency nanocomposite sorbents for CO<sub>2</sub> capture based on amine-functionalized mesoporous capsules. *Energy Environ. Sci.* **4**, 444–452 (2011).
- Ferey, G. A Chromium Terephthalate-Based Solid with Unusually Large Pore Volumes and Surface Area. *Science* **309**, 2040–2042 (2005).
- Hwang, Y. K. *et al.* Amine grafting on coordinatively unsaturated metal centers of MOFs: Consequences for catalysis and metal encapsulation. *Angew. Chem. Int. Edit.* **47**, 4144–4148 (2008).
- Hong, D. Y., Hwang, Y. K., Serre, C., Ferey, G. & Chang, J. S. Porous Chromium Terephthalate MIL-101 with Coordinatively Unsaturated Sites: Surface Functionalization, Encapsulation, Sorption and Catalysis. *Adv. Funct. Mater.* **19**, 1537–1552 (2009).
- Gascon, J., Serra-Crespo, P., Ramos-Fernandez, E. V. & Kapteijn, F. Synthesis and Characterization of an Amino Functionalized MIL-101(Al): Separation and Catalytic Properties. *Chem. Mater.* **23**, 2565–2572 (2011).
- Xu, X. C., Song, C. S., Andresen, J. M., Miller, B. G. & Scaroni, A. W. Preparation and characterization of novel CO<sub>2</sub> "molecular basket" adsorbents based on polymer-modified mesoporous molecular sieve MCM-41. *Micropor. Mesopor. Mat.* **62**, 29–45 (2003).
- Chowdhury, P., Bikkina, C. & Gumma, S. Gas Adsorption Properties of the Chromium-Based Metal Organic Framework MIL-101. *J. Phys. Chem. C* **113**, 6616–6621 (2009).
- Liu, Y. Y., Ju-Lan, Z., Jian, Z., Xu, F. & Sun, L. X. Improved hydrogen storage in the modified metal-organic frameworks by hydrogen spillover effect. *Int. J. Hydrogen Energy* **32**, 4005–4010 (2007).
- Bollini, P., Didas, S. A. & Jones, C. W. Amine-oxide hybrid materials for acid gas separations. *J. Mater. Chem.* **21**, 15100–15120 (2011).
- Choi, S., Drese, J. H., Eisenberger, P. M. & Jones, C. W. Application of Amine-Tethered Solid Sorbents for Direct CO<sub>2</sub> Capture from the Ambient Air. *Environ. Sci. Technol.* **45**, 2420–2427 (2011).
- Sips, R. On the Structure of a Catalyst Surface.2. *J. Chem. Phys.* **18**, 1024–1026 (1950).
- Sips, R. On the Structure of a Catalyst Surface. *J. Chem. Phys.* **16**, 490–495 (1948).
- An, J. & Rosi, N. L. Tuning MOF CO<sub>2</sub> Adsorption Properties via Cation Exchange. *J. Am. Chem. Soc.* **132**, 5578–5579 (2010).
- McDonald, T. M., D'Alessandro, D. M., Krishna, R. & Long, J. R. Enhanced carbon dioxide capture upon incorporation of N,N'-dimethylethylenediamine in the metal-organic framework CuBTTri. *Chem. Sci.* **2**, 2022–2028 (2011).
- McDonald, T. M. *et al.* Capture of Carbon Dioxide from Air and Flue Gas in the Alkylamine-Appended Metal-Organic Framework mmen-Mg<sub>2</sub>(dobpdc). *J. Am. Chem. Soc.* **134**, 7056–7065 (2012).
- Granite, E. J. & Pennline, H. W. Photochemical removal of mercury from flue gas. *Ind. Eng. Chem. Res.* **41**, 5470–5476 (2002).
- Peeters, A. N. M., Faaij, A. P. C. & Turkenburg, W. C. Techno-economic analysis of natural gas combined cycles with post-combustion CO<sub>2</sub> absorption, including a



- detailed evaluation of the development potential. *Int. J. Greenh. Gas. Con.* **1**, 396–417 (2007).
33. Bloch, E. D. *et al.* Metal Insertion in a Microporous Metal-Organic Framework Lined with 2,2'-Bipyridine. *J. Am. Chem. Soc.* **132**, 14382–14384 (2010).
34. Lu, W. G. *et al.* Sulfonate-Grafted Porous Polymer Networks for Preferential CO<sub>2</sub> Adsorption at Low Pressure. *J. Am. Chem. Soc.* **133**, 18126–18129 (2011).
35. Liu, Y., Wang, Z. U. & Zhou, H.-C. Recent advances in carbon dioxide capture with metal-organic frameworks. *Greenh. Gas.: Sci. and Technol.* **2**, 239–259 (2012).
36. Farha, O. K. *et al.* De novo synthesis of a metal-organic framework material featuring ultrahigh surface area and gas storage capacities. *Nat. Chem.* **2**, 944–948 (2010).
37. Chae, H. K. *et al.* A route to high surface area, porosity and inclusion of large molecules in crystals. *Nature* **427**, 523–527 (2004).

## Acknowledgments

We gratefully acknowledge the financial support by the national key basic research program of China (Grant No. 2012CB722700), national science foundation of China (Grant No.51072204, 51172249) and the aided program for science and technology innovative research team of Ningbo municipality (Grant No.2009B21005).

## Author contributions

L.C., C.K. and Y.L. designed the project; Y.L. carried out the experiments; Y.L. wrote the manuscript. All authors discussed the results and commented on the manuscript.

## Additional information

**Supplementary information** accompanies this paper at <http://www.nature.com/scientificreports>

**Competing financial interests:** The authors declare no competing financial interests.

**License:** This work is licensed under a Creative Commons Attribution-NonCommercial-ShareAlike 3.0 Unported License. To view a copy of this license, visit <http://creativecommons.org/licenses/by-nc-sa/3.0/>

**How to cite this article:** Lin, Y., Yan, Q., Kong, C. & Chen, L. Polyethyleneimine Incorporated Metal-Organic Frameworks Adsorbent for Highly Selective CO<sub>2</sub> Capture. *Sci. Rep.* **3**, 1859; DOI:10.1038/srep01859 (2013).